

# Design and Synthesis of Highly Photostable Yellow–Green Emitting 1,8-Naphthalimides as Fluorescent Sensors for Metal Cations and Protons

Vladimir B. Bojinov · Nikolai I. Georgiev · Paula Bosch

Received: 16 April 2008 / Accepted: 20 June 2008 / Published online: 30 July 2008  
© Springer Science + Business Media, LLC 2008

**Abstract** Two highly photostable yellow–green emitting 1,8-naphthalimides **5** and **6**, containing both *N*-linked hindered amine moiety and a secondary or tertiary cation receptor, were synthesized for the first time. Novel compounds were configured as “fluorophore–spacer–receptor” systems based on photoinduced electron transfer. Photo-physical characteristics of the dyes were investigated in DMF and water/DMF (4:1, *v/v*) solution. The ability of the new compounds to detect cations was evaluated by the changes in their fluorescence intensity in the presence of metal ions ( $\text{Cu}^{2+}$ ,  $\text{Pb}^{2+}$ ,  $\text{Zn}^{2+}$ ,  $\text{Ni}^{2+}$ ,  $\text{Co}^{2+}$ ) and protons. The presence of metal ions and protons was found to disallow a photoinduced electron transfer leading to an enhancement in the dye fluorescence intensity. Compound **5**, containing secondary amine receptor, displayed a good sensor activity towards metal ions and protons. However the sensor activity of dye **6**, containing a tertiary amine receptor and a shorter hydrocarbon spacer, was substantially higher. The results obtained indicate the potential of the novel compounds as highly photostable and efficient “off–on” pH switchers and fluorescent detectors for metal ions with pronounced selectivity towards  $\text{Cu}^{2+}$  ions.

**Keywords** 1,8-Naphthalimide · Fluorescence · Hindered amine light stabilizers · Photostability · Metal and proton sensors · Photoinduced electron transfer

## Abbreviation

HALS hindered amine light stabilizer  
PET photoinduced electron transfer

## Introduction

The area of molecular devices has advanced considerably during the past few years. The extension of the concept of a device to the molecular level is of interest, not only for basic research, but also for the growth of nanoscience and the development of nanotechnology [1]. Supramolecular devices that show large changes in their so called “off” and “on” states are currently of great interest as these can be modulated, or tuned, by employing external sources such as ions, molecules, light, etc. [2, 3]. The “off” and “on” states of the molecular-level devices refer to their luminescence, magnetic or electronic properties. Luminescence is one of the most useful techniques to monitor the operation of molecular devices. A part of this rapidly emerging field is the development of fluorescent sensors where the fluorescence is switched “off” or “on” as a function of the analyte [4–7].

The photoinduced electron transfer (PET) system using the “fluorophore–spacer–receptor” format, developed by de Silva [8], is one of the most popular approaches to the design of fluorescent sensors and switchers [9]. In this model, the excited state of the fluorophore can be quenched by intermolecular electron transfer from the receptor to the

V. B. Bojinov (✉) · N. I. Georgiev  
Department of Organic Synthesis,  
University of Chemical Technology and Metallurgy,  
Kliment Ohridsky 8,  
1756 Sofia, Bulgaria  
e-mail: vlbojinov@uctm.edu

P. Bosch  
Institute of Science and Technology of Polymers, CSIC,  
Juan de la Cierva 3,  
28006 Madrid, Spain

fluorophore (or vice versa) prior recognition. Upon recognition of species such as cations, the oxidation potential of the receptor is increased and this causes the electron transfer to be “switched off” and in turn the emission to be “switched on” [10–12].

Naphthalimide derivatives are a special class of environmentally sensitive fluorophores [13–15]. Because of their strong yellow–green fluorescence and good photostability, the 4-amino-1,8-naphthalimide derivatives have found application in a number of areas including coloration of polymers [16–22], laser active media [23, 24], potential photosensitive biologically units [25], fluorescent markers in biology [26], light emitting diodes [27, 28], fluorescence sensors and switches [29–34], electroluminescent materials [35–37], liquid crystal displays [38, 39] and ion probes [40]. Moreover, these properties are essential when employing such devices in real-time and on-line analysis.

Recently we have synthesized new polymerizable yellow–green emitting 1,8-naphthalimides, containing a hindered amine light stabilizer (HALS) fragment, designed as highly photostable additives for “one-step” fluorescent dyeing and photostabilization of polymers [17, 32]. These results encouraged our efforts towards the design and synthesis of novel photostable 1,8-naphthalimide fluorescence sensors, *N*-substituted with a hindered amine moiety. 2,2,6,6-Tetramethylpiperidine and *N*-methylpiperazine units were incorporated in the 1,8-naphthalimide C-4 position as a cation receptor. This paper takes on added significance given the growing body of sensors and other optical devices which employ 4-amino-1,8-naphthalimide fluorophores. Hence, compounds **5** and **6** (Scheme 1) were synthesized and investigated by electronic absorption and emission

spectroscopy as potential PET sensors for protons and transition metal ions.

In order to receive a more complete comparative picture for the influence of a HALS fragment on the properties of the examined compounds, previously synthesized 1,8-naphthalimide compound **8** [17], not containing a receptor moiety at C-4 position, as well as 1,8-naphthalimide fluorophores **10** [17] and **11** [41], not possessing *N*-linked HALS fragment in their molecules were involved in the present study as reference compounds (Scheme 2).

## Experimental

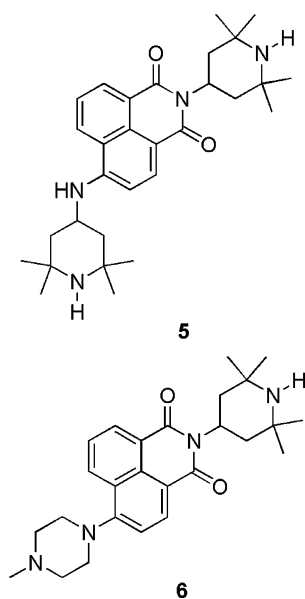
### Materials

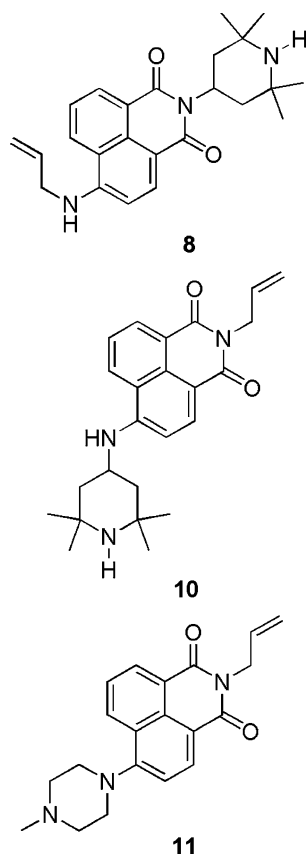
Reference 1,8-naphthalimides **8**, **10** [17, 32] and **11** [41], as well as starting 4-nitro-1,8-naphthalic anhydride **1** [36] were synthesized according to the procedures described before. 2,2,6,6-Tetramethylpiperidin-4-ylamine **2**, *N*-methylpiperazine **4** and allylamine **7** (Fluka, Aldrich), p.a. grade, was used without purification. All solvents (Fluka, Merck) were of p.a. or analytical grade.  $\text{Zn}(\text{NO}_3)_2$ ,  $\text{Cu}(\text{NO}_3)_2$ ,  $\text{Ni}(\text{NO}_3)_2$ ,  $\text{Co}(\text{NO}_3)_2$  and  $\text{Pb}(\text{NO}_3)_2$  salts were the sources for metal cations. To adjust the pH, very small volumes of sulphuric acid and sodium hydroxide were used. The effect of the metal cations and protons upon the fluorescence intensity was examined by adding 10  $\mu\text{l}$  portions of the metal cations stock solution ( $3.33 \times 10^{-6} \text{ mol l}^{-1}$ ) to a known volume of the fluorophore solution (3 ml). The addition was limited to 0.09 ml so that dilution remains insignificant.

### Methods

FT-IR spectra were recorded on a Bruker IFS-113 spectrometer at  $2 \text{ cm}^{-1}$  resolution using KBr discs. The  $^1\text{H}$  NMR spectra were recorded on a Bruker DRX-250 spectrometer, operating at 250.13 MHz. The measurements were carried out in  $\text{DMSO-}d_6$  solution at ambient temperature. The chemical shifts (given as  $\delta$  in ppm) were referenced to tetramethylsilane (TMS) standard. UV/vis spectra were recorded on a Hewlett Packard 8452A spectrophotometer with 2 nm resolution at room temperature. The fluorescence spectra were taken on a Perkin Elmer LS 45 fluorescence spectrophotometer. The fluorescence quantum yields ( $\Phi_{\text{F}}$ ) were measured relatively to Coumarin 6 ( $\Phi_{\text{ref}}=0.78$  in ethanol) [42]. TLC was performed on silica gel, Fluka F60 254,  $20 \times 20$ , 0.2 mm, using as eluant the solvent system chloroform/methanol (3:2). The melting points were determined by means of a Kofler melting point microscope.

**Scheme 1** Compounds **5** and **6**



**Scheme 2** Compounds **8**, **10** and **11**

### Synthesis of 1,8-naphthalimides (**5**) and (**6**)

To a suspension of 4-nitro-1,8-naphthalenedicarboxylic acid anhydride **1** (2.43 g, 10 mmol) in 40 ml of ethanol, a solution of 1.56 g of 2,2,6,6-tetramethylpiperidin-4-ylamine **2** ( $d=0.91$ , 10 mmol) in 10 ml of ethanol was added dropwise under stirring at ambient temperature over a period of 30 min. The resulting mixture was stirred at 60 °C for 4 h. The crude product that precipitated on cooling was treated with 50 ml of 5% aqueous sodium hydroxide to give after filtration, washing with water and drying 3.51 g (92%) of pure 4-nitro-*N*-(2,2,6,6-tetramethylpiperidin-4-yl)-1,8-naphthalimide **3** as pale yellow crystals (m.p. 199–201 °C). To a solution of intermediate **3** (1.91 g, 5 mmol) in 50 ml of DMF, 5 mmol of appropriate amine (0.78 g of 2,2,6,6-tetramethylpiperidine-4-ylamine **2** or 0.50 g of *N*-methylpiperazine **4**) was added at room temperature. After 24 h (TLC control in a solvent system chloroform/methanol=3:2), the resulting solution was poured into 300 ml of water. The precipitate was filtered off and washed with water. The crude product was dissolved in a hot mixture solvent of water (5 ml) and ethanol (100 ml), and the undissolved residue was filtered off. The filtrate then was diluted in 100 ml of water and the precipitated product was filtered off and dried. Recrystallization from ethanol-water (30:70,  $v/v$ ) afforded

1.84 g (75%) of 4-(2,2,6,6-tetramethylpiperidin-4-ylamino)-*N*-(2,2,6,6-tetramethylpiperidin-4-yl)-1,8-naphthalimide **5** or 1.72 g (79%) of 4-(4-methylpiperazin-1-yl)-*N*-(2,2,6,6-tetramethylpiperidin-4-yl)-1,8-naphthalimide **6** as yellow-orange crystals.

4-(2,2,6,6-Tetramethylpiperidin-4-ylamino)-*N*-(2,2,6,6-tetramethylpiperidin-4-yl)-1,8-naphthalimide (**5**) FT-IR (KBr)  $\text{cm}^{-1}$ : 3,438, 3,382 и 3,246 ( $\nu\text{NH}$ ); 2,912 ( $\nu\text{CH}_3$ ); 1,692 ( $\nu^{\text{as}}\text{N}-\text{C}=\text{O}$ ); 1,656 ( $\nu^{\text{s}}\text{N}-\text{C}=\text{O}$ ).  $^1\text{H}$  NMR (DMSO- $d_6$ , 250.13 MHz) ppm: 8.66 (d, 1H,  $J=8.2$  Hz, naphthalimide 7-H); 8.39 (d, 1H,  $J=7.2$  Hz, naphthalimide 5-H); 8.22 (d, 1H,  $J=8.4$  Hz, naphthalimide 2-H); 7.69 (m, 2H, naphthalimide 5-H and ArNH); 6.77 (d, 1H,  $J=8.4$  Hz, naphthalimide 3-H); 5.54 (m, 1H, piperidine (CO) $_2$ NHCH); 4.08 (m, 1H, piperidine ArNHCH); 2.40 (t, 2H,  $J=11.9$  Hz, piperidine CH $_2$ ); 1.71 (m, 3H, piperidine NH and CH $_2$ ); 1.42 (m, 5H, piperidine NH and 2 $\times$ CH $_2$ ); 1.23 (s, 12H, piperidine 2 $\times$ CH $_3$ ); 1.20 (s, 12H, piperidine 2 $\times$ CH $_3$ ); 1.09 (s, 12H, piperidine 2 $\times$ CH $_3$ ); 1.04 (s, 12H, piperidine 2 $\times$ CH $_3$ ). Analysis: Calculated for (%) C $_{30}$ H $_{42}$ N $_4$ O $_2$  (MW 490.68) C 73.43, H 8.63, N 11.42; Found (%) C 73.71, H 8.55, N 11.30.

4-(4-Methylpiperazin-1-yl)-*N*-(2,2,6,6-tetramethylpiperidin-4-yl)-1,8-naphthalimide (**6**) FT-IR (KBr)  $\text{cm}^{-1}$ : 3,308 ( $\nu\text{NH}$ ); 2,860 ( $\nu\text{CH}_3$ ); 1,690 ( $\nu^{\text{as}}\text{N}-\text{C}=\text{O}$ ); 1,652 ( $\nu^{\text{s}}\text{N}-\text{C}=\text{O}$ ).  $^1\text{H}$  NMR (DMSO- $d_6$ , 250.13 MHz) ppm: 8.67 (d, 1H,  $J=8.4$  Hz, naphthalimide 7-H); 8.39 (d, 1H,  $J=7.3$  Hz, naphthalimide 5-H); 8.21 (d, 1H,  $J=8.5$  Hz, naphthalimide 2-H); 7.65 (t, 1H,  $J=7.9$  Hz, naphthalimide 5-H); 7.32 (d, 1H,  $J=8.5$  Hz, naphthalimide 3-H); 5.53 (m, 1H, piperidine (CO) $_2$ NHCH); 3.17 (t, 4H,  $J=12.5$  Hz, piperazine 2 $\times$  ArNHCH $_2$ ); 2.72 (t, 4H,  $J=12.4$  Hz, piperazine 2 $\times$ CH $_2$ NMe); 2.40 (t, 2H,  $J=12.1$  Hz, piperidine CH $_2$ ); 2.10 (s, 3H, piperazine NMe); 1.43 (dd, 2H,  $J=12.1$  Hz,  $J=2.3$  Hz, piperidine CH $_2$ ); 1.22 (s, 12H, piperidine 2 $\times$ CH $_3$ ); 1.07 (s, 12H, piperidine 2 $\times$ CH $_3$ ). Analysis: Calculated for (%) C $_{26}$ H $_{34}$ N $_4$ O $_2$  (MW 434.57) C 71.86, H 7.89, N 12.89; Found (%) C 71.61, H 7.78, N 13.01.

### Photodegradation of dyes

The study on the photodegradation of the fluorescent dyes was conducted in a solar simulator SUNTEST CPS equipment (Heraeus, Germany), supplied with an arc air-cooled Xenon lamp (Hanau, 1.1 kW, 765 W m $^{-2}$ ), at ambient temperature. The irradiation of dyes was performed in DMF solution at concentration 10 $^{-5}$  mol l $^{-1}$ . The changes in dye concentration were followed spectrophotometrically by the changes of the absorption maxima in the

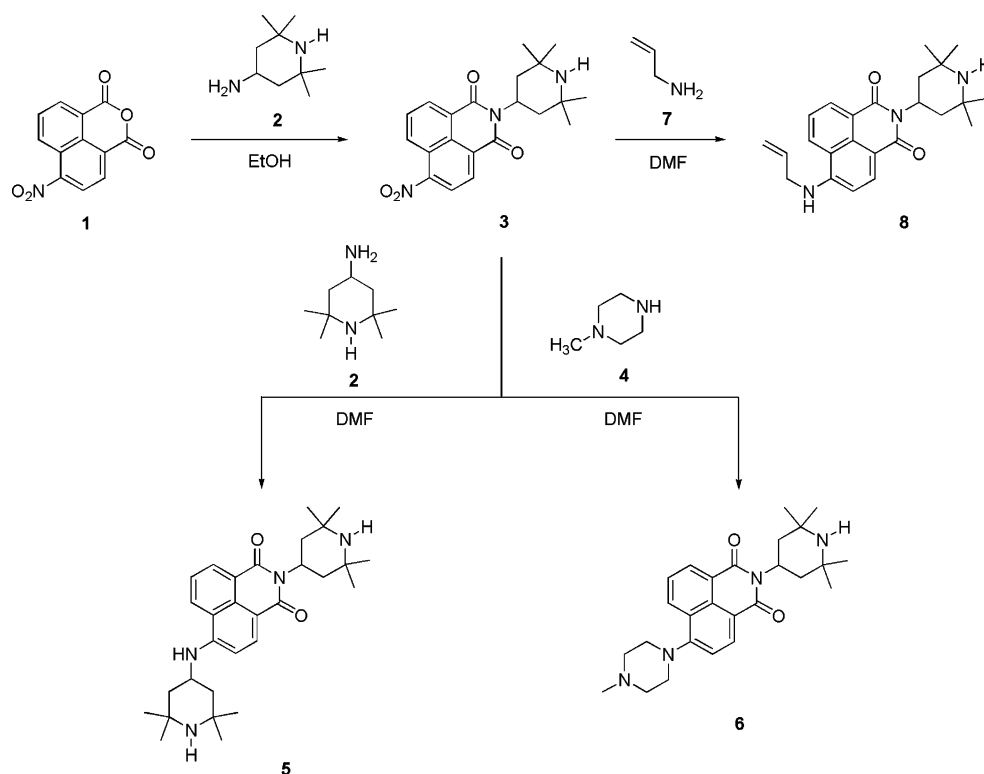
visible region using the method of a standard calibration curve.

## Results and discussion

### Design of the dyes

The two dyes (**5** and **6**) were designed to act as photostable detectors of environment pollution by transition metal cations and protons. They are configured on the “fluorophore–spacer–receptor” model, where the 4-amino-1,8-naphthalimide moiety is the fluorophore and the 2,2,6,6-tetramethylpiperidin-4-yl amine or 4-methylpiperazine *N*-amine in the C-4 substituent is the analyte receptor. The hydrocarbon part of the piperidine and piperazine fragments serve as spacer that covalently separates the two units. In these particular cases, it was predicted that a PET process (an electron transfer from the receptor to the excited state of the fluorophore) would quench fluorescence emission of the 1,8-naphthalimide unit. This would represent the “off-state” of the system. The protonation or respective metal complex formation of the piperidine amine or piperazine *N*-amine would increase the oxidation potential of the receptor, and as such, thermodynamically disallow the electron transfer [43, 44]. Consequently the emission would be “switched on”. Thus, we expect the fluorescence to be strong in acidic media and transition metal cations environment.

**Scheme 3** Synthesis of the novel dyes **5** and **6** performed in two steps



### Synthesis

The synthesis of the novel dyes **5** and **6** was performed in two steps as it is shown in Scheme 3. First, the intermediate **3** was obtained by condensation of 2,2,6,6-tetramethylpiperidin-4-ylamine **2** with 4-nitro-1,8-naphthalic anhydride **1** in ethanol at 60 °C for 4 h. In order to obtain the target fluorescent 1,8-naphthalimides **5** and **6**, the nitro group in the intermediate **3** was nucleophilically substituted with the commercially available 2,2,6,6-tetramethylpiperidin-4-ylamine **2** or *N*-methylpiperazine **4**, respectively, in DMF at room temperature for 24 h.

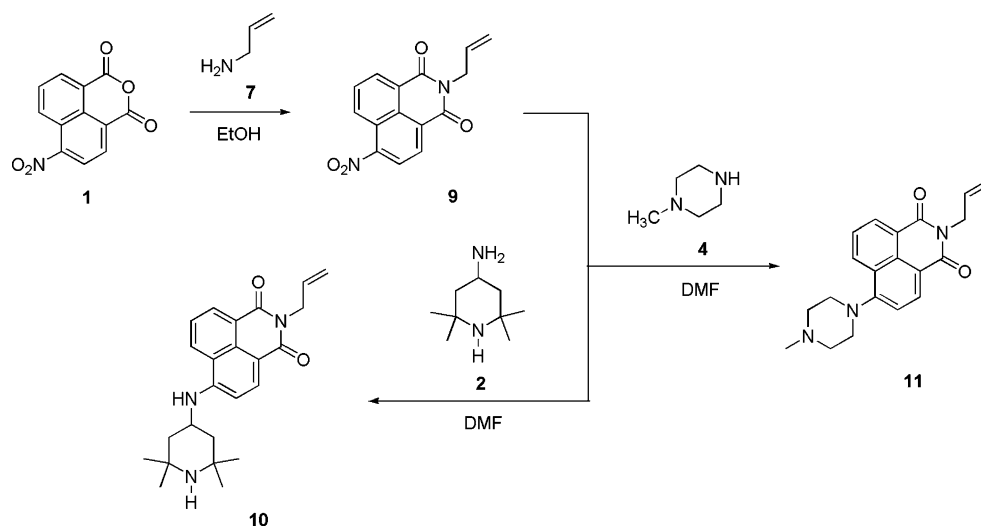
The reference compound **8** was synthesized as before [17] by the same procedure, whereupon allylamine **7** was used in the second step instead of 2,2,6,6-tetramethylpiperidin-4-ylamine **2** or *N*-methylpiperazine **4** (Scheme 3).

The synthesis of reference dyes **10** and **11** was carried out in two steps as well (Scheme 4) as described before [17, 41]. However, initially 4-nitro-1,8-naphthalic anhydride **1** was reacted with allylamine **7**, then the intermediate **9** was transformed in the final dyes by substitution of the nitro group with 2,2,6,6-tetramethylpiperidin-4-ylamine or *N*-methylpiperazine unit.

The synthesized compound was fully characterized by melting point, TLC ( $R_f$  value), UV/vis (Table 1) and fluorescence spectra and identified by elemental analysis data, FT-IR and  $^1\text{H}$  NMR spectra.

The structures and purities of the desired products were confirmed by conventional techniques. For instance, in the

**Scheme 4** Synthesis of reference dyes **10** and **11** carried out in two steps



$^1\text{H}$  NMR ( $\text{DMSO-}d_6$ , 250.13 MHz) spectra of novel compounds **5** and **6** a resonance at 6.77 ppm (**5**) and 7.32 ppm (**6**) was observed. These are characteristic for the proton in position C-3 of the 1,8-naphthalimide ring, substituted in position C-4 with an electron-donating 2,2,6,6-tetramethylpiperidine or *N*-methylpiperazine group respectively. Furthermore, the  $^1\text{H}$  NMR spectra contained peaks, attributed to the protons for 2,2,6,6-tetramethylpiperidine and *N*-methylpiperazine moieties.

Photophysical characterization of the dyes

The light absorption properties of the 4-substituted-1,8-naphthalimides under study are basically related to the polarization of the 1,8-naphthalimide molecule on irradiation, resulting from the electron donor-acceptor interaction between the substituent at C-4 position and the carbonyl groups of the chromophoric system, and may be influenced by the environmental effect of the media. In DMF solution the longest-wavelength absorption maximum of piperazine substituted 1,8-naphthalimides (compounds **6** and **11**)

appears in the visible region at  $\lambda_A=402\text{--}406$  nm, while the corresponding absorption maxima of 4-(2,2,6,6-tetramethylpiperidine)-1,8-naphthalimides **5**, **8** and **10** are bathochromically shifted to  $\lambda_A=432\text{--}436$  nm (Fig. 1), which is surely connected with the different electron-donating ability of the piperazine and 4-amino-piperidine moieties at the 1,8-naphthalimide C-4 position. This could be due to the stronger repulsive interaction between the amine receptor and 4-amino moiety in the case of compound **6** (tertiary amines and shorter hydrocarbon spacer), which destabilizes the ICT excited state nature of this compound to the larger extent, resulting in more energy being required to access the excited state. The dyes' molar absorptivity ( $\epsilon$ ) in the longest-wavelength band of the absorption spectra is higher than  $10,000$   $\text{l mol}^{-1} \text{cm}^{-1}$  (Table 1), indicating that this is a charge transfer (CT) band, due to ( $\pi,\pi^*$ ) character of the  $S_0\rightarrow S_1$  transition.

Basic fluorescent characteristics of novel dyes (**5** and **6**) and reference compounds (**8**, **10** and **11**) such as the fluorescence ( $\lambda_F$ ) maxima, Stokes shift ( $\nu_A-\nu_F$ ), oscillator

**Table 1** Yields, melting points, retention factors and absorption data for 1,8-naphthalimides **5**, **6**, **8**, **10** and **11** in DMF solution

Compound	Yield (%)	Mp ( $^{\circ}\text{C}$ )	$\lambda_A$ (nm)	$\log \epsilon$ ( $\text{l mol}^{-1} \text{cm}^{-1}$ )	
<b>5</b>	75	193–195	0.13	434	4.224
<b>6</b>	79	188–190	0.19	406	4.086
<b>8</b>	86	140–142 <sup>b</sup>	0.25	432	4.289
<b>10</b>	78	137–139 <sup>b</sup>	0.23	436	4.170
<b>11</b>	76	146–148 <sup>c</sup>	0.44	402	4.027

<sup>a</sup> TLC in a solvent system chloroform/methanol (3:2)

<sup>b</sup> Melting points of compounds **8** (141–143  $^{\circ}\text{C}$ ) and **10** (136–138  $^{\circ}\text{C}$ ) according reference [32]

<sup>c</sup> Melting point of compound **11** (147–149  $^{\circ}\text{C}$ ) according reference [41]

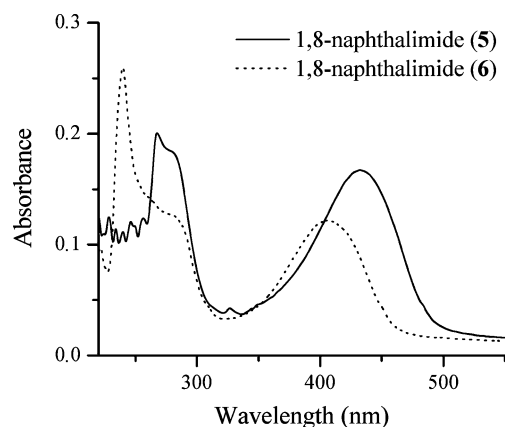


**Fig. 1** Absorption spectra of novel 1,8-naphthalimides **5** and **6** in DMF solution at concentration  $10^{-5} \text{ mol l}^{-1}$

strength ( $f$ ), fluorescent both quantum ( $\Phi_F$ ) and energy ( $E_F$ ) yields were measured in DMF solution and presented in Table 2.

In DMF solution all compounds under study displayed yellow–green fluorescence due to the charge transfer in the 1,8-naphthalimide moieties from the electron-donating alkylamino group at C-4 position to the carbonyl groups. The dyes' emission was observed in the visible region with well-pronounced maxima ( $\lambda_F$ ) at 525–532 nm. Figure 2 displays the absorption and fluorescence spectra of the fluorescent dye **5** as a typical example for the spectra of compounds under study.

The fluorescence curve is approximately mirror image of the absorption one. This indicates preservation of the fluorophore molecular structure in the excited state. The overlap between absorption and fluorescence bands is small and an aggregation effect at concentration of  $10^{-5}$  mol  $\text{l}^{-1}$  has not been observed.

The Stokes shift ( $\nu_A - \nu_F$ ) and oscillator strength ( $f$ ) are important characteristics for the fluorescent compounds. The Stokes shift is a parameter that indicates the difference in the properties and structure of the fluorophores between the ground state  $S_0$  and the first excited state  $S_1$ . The Stokes shifts ( $\text{cm}^{-1}$ ) were calculated by Eq. 1:

$$(\nu_A - \nu_F) = \left( \frac{1}{\lambda_A} - \frac{1}{\lambda_F} \right) \times 10^7. \quad (1)$$

The Stokes shift values of the piperazine substituted 1,8-naphthalimides **6** and **11** ( $5,619$ – $5,828$   $\text{cm}^{-1}$ ) were higher than those of the 4-(2,2,6,6-tetramethylpiperidine)-1,8-naphthalimides **5**, **8** and **10** ( $4,138$ – $4,244$   $\text{cm}^{-1}$ ). As the dipole moment of the molecule is enhanced upon excitation due to electron density redistribution, the excited molecule is better stabilized in polar solvents, such as DMF, because of stronger interaction with the solvent dipoles [45]. This effect causes the red shift in the fluorescence maxima resulting in large-scale augmentation of the Stokes shift values for piperazine substituted 1,8-naphthalimides.

The oscillator strength ( $f$ ) shows the effective number of electrons whose transition from ground to excited state gives the absorption area in the electron spectrum. Values

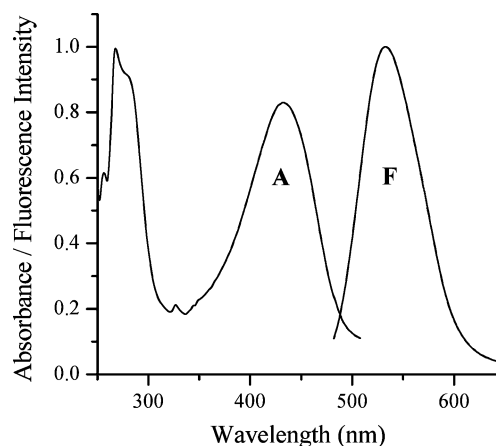


**Fig. 2** Normalized absorption ( $\lambda_A$ ) and fluorescence ( $\lambda_F$ ) spectra of dye **5** in DMF solution at concentration  $10^{-5}$  mol  $\text{l}^{-1}$

of the oscillator strength were calculated using Eq. 2 where  $\Delta\nu_{1/2}$  is the width of the absorption band ( $\text{cm}^{-1}$ ) at  $1/2$  ( $\epsilon_{\max}$ ) [46]:

$$f = 4.32 \times 10^{-9} \Delta\nu_{1/2} \epsilon_{\max}. \quad (2)$$

The oscillator strength values for the 1,8-naphthalimide dyes under study were in range  $0.175$ – $0.385$ , which is in accordance with the data for other similar 1,8-naphthalimide derivatives [47, 48].

The ability of the molecules to emit the absorbed light energy is characterized quantitatively by the fluorescence quantum yield ( $\Phi_F$ ). The quantum yields of fluorescence were calculated relatively to Coumarin 6 ( $\Phi_{\text{ref}}=0.78$ ) as a reference compound [42] according to Eq. 3, where  $A_{\text{ref}}$ ,  $S_{\text{ref}}$ ,  $n_{\text{ref}}$  and  $A_{\text{sample}}$ ,  $S_{\text{sample}}$ ,  $n_{\text{sample}}$  represent the absorbance at the excited wavelength, the integrated emission band area and the solvent refractive index of the standard and the sample, respectively:

$$\Phi_F = \Phi_{\text{ref}} \left( \frac{S_{\text{sample}}}{S_{\text{ref}}} \right) \left( \frac{A_{\text{ref}}}{A_{\text{sample}}} \right) \left( \frac{n_{\text{sample}}^2}{n_{\text{ref}}^2} \right). \quad (3)$$

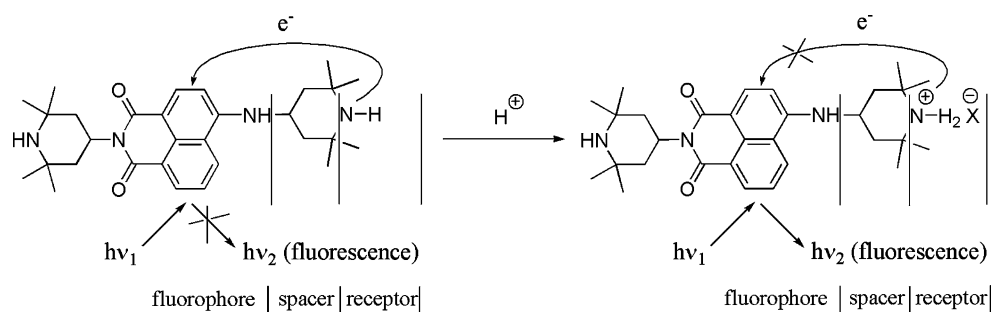
The energy yield of fluorescence  $E_F$  (Table 1), calculated by Eq. 4, could also be used instead of  $\Phi_F$  [49]:

$$E_F = \Phi_F \frac{\lambda_A}{\lambda_F}. \quad (4)$$

As can be seen from the data presented in Table 2, the quantum yield of fluorescence of 1,8-naphthalimides **5**, **6**, **10** and **11**, possessing 2,2,6,6-tetramethylpiperidine or *N*-methylpiperazine unit at C-4 position, are vastly lower in respect to those of traditional yellow–green emitting 1,8-naphthalimides, not containing PET receptor [39, 47] and lower to that of 1,8-naphthalimide **8**, not containing such a “lower” moiety. On the other hand, the quantum yield of fluorescence of 1,8-naphthalimides **6** and **11**, containing tertiary amine receptor, was lower than those of dyes **5** and

**Table 2** Fluorescence characteristics of dyes **5**, **6**, **8**, **10** and **11** in DMF solution at concentration  $10^{-5}$  mol  $\text{l}^{-1}$  ( $\lambda_{\text{ex}}=\lambda_A$ )

Compound	$\lambda_{\text{ex}}$ (nm)	$\lambda_F$ (nm)	$\nu_A - \nu_F$ ( $\text{cm}^{-1}$ )	$f$	$\Phi_F$	$E_F$
<b>5</b>	434	532	4,244	0.332	0.118	0.080
<b>6</b>	406	526	5,619	0.213	0.049	0.038
<b>8</b>	432	528	4,209	0.385	0.383	0.313
<b>10</b>	436	532	4,138	0.297	0.124	0.093
<b>11</b>	402	525	5,828	0.175	0.052	0.040

**Scheme 5** Quenching of the fluorescence of the 4-amino-1,8-naphthalimide fluorophore

**10.** This phenomenon might be caused by the possible photoinduced electron transfer from the piperidine or *N*-methylpiperazine amine donor (receptor) to the 4-amino-1,8-naphthalimide fluorophore through the saturated piperidinyl (piperazinyl) ring. Thus the fluorescence of the 4-amino-1,8-naphthalimide fluorophore is quenched (Scheme 5). Upon recognition of the analyte (protons or transition metal ion) piperidine (*N*-methylpiperazine) amine would increase the oxidation potential of the receptor, and as such, thermodynamically disallow the electron transfer and the emission would be “switched on” [43, 44].

Furthermore, as demonstrated experimentally by de Silva et al., only the receptor that is directly attached to the 4-amino moiety (the “lower” moiety) is capable of quenching the fluorophores excited state [43]. This is due to the fact that molecules like 1,8-naphthalimides under study have high excited state dipole moments that arise from their internal charge transfer (ICT) excited state nature. In this case the amino moiety is acting as an electron donor, whereas the imide functions as an electron acceptor. Consequently, a push–pull mechanism is in operation, and due to charge repulsion, disallows the “upper” amine (compound **8**) to transfer an electron to the naphthalimide excited state [50].

The results obtained suppose PET sensor properties of the fluorescent dyes **5**, **6**, **10** and **11**, containing “lower” 4-aminopiperidine (**5** and **10**) or *N*-methylpiperazine (**6** and **11**) moiety at C-4 position of the 1,8-naphthalimide fluorophore, which was the reason to investigate their photophysical behaviour in water/DMF (4:1, *v/v*) at different pH values and in the presence of transition metal ions.

Influence of pH on the fluorescence properties of the dyes

The photophysical characteristics of the dyes in distilled water/DMF (4:1, *v/v*) solution are represented in Table 3. Some bathochromic shift of the absorption and fluorescence maxima of the compounds was observed if compared spectra to those recorded in DMF. The oscillator strength values calculated in water/DMF (4:1, *v/v*) were higher than those in DMF which is well correlated with the increase in the extinction coefficient of the dyes in this medium.

As a typical example for all compounds under study, when the absorption spectra of novel dyes **5** and **6** were recorded in alkaline solution at ca. pH 11.3, an absorption band was observed in range 340–530 nm for compound **5** and 330–490 nm for compound **6** due to the ICT state, with  $\lambda_A$  maximum at 446 and 420 nm respectively (Fig. 3). Upon acidification the band was blue shifted with small reductions in its maximum intensity at ca. pH 6.6. However, upon further acidification (ca. pH 2.2) the  $\lambda_A$  became further blue shifted with small intensity enhancements. These changes can however, be considered to be only minor in comparison to the changes in the fluorescence spectra (vide infra). The reason for the blue shift is twofold. First, the protonation of the amine receptor will exert some weak charge repulsion on the 4-amino moiety of the fluorophores. However, the major reason is that in very acidic conditions the push–pull character of the ICT state is partially reduced due to the protonation of the 4-amino moiety itself [50].

Family of fluorescence emission spectra of the dyes as a function of pH were recorded in water/DMF (4:1, *v/v*) and plotted in Fig. 4. 4-Allylamino-1,8-naphthalimide **8**, which

**Table 3** Absorption and fluorescence characteristics ( $\lambda_{\text{ex}}=\lambda_A$ ) of 1,8-naphthalimides **5**, **6**, **8**, **10** and **11** at concentration  $10^{-5}$  mol  $\text{l}^{-1}$  in water/DMF (4:1, *v/v*)

Compound	$\lambda_A$ (nm)	$\log \epsilon$ ( $1 \text{ mol}^{-1} \text{ cm}^{-1}$ )	$\lambda_F$ (nm)	$\nu_A-\nu_F$ ( $\text{cm}^{-1}$ )	$f$	FE <sup>a</sup>	pK <sub>a</sub>
<b>5</b>	440	4.339	539	4,174	0.433	4.72	7.26
<b>6</b>	414	4.211	534	5,428	0.284	41.89	6.92
<b>8</b>	440	4.398	537	4,105	0.495	1.29	-
<b>10</b>	442	4.301	540	4,106	0.402	3.91	7.37
<b>11</b>	410	4.156	533	5,629	0.236	36.33	6.96

<sup>a</sup> Factor for proton-induced fluorescence enhancement  $FE=I_{F\text{max}}/I_{F\text{min}}$  ( $I_F$ —fluorescence intensity, arbitrary units)

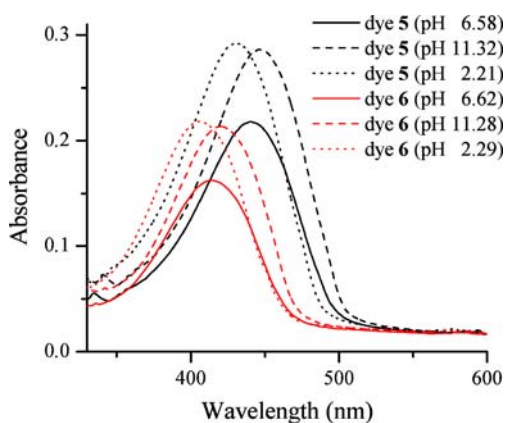


**Fig. 3** Absorption spectra of 1,8-naphthalimides **5** and **6** (concentration  $10^{-5}$  mol  $l^{-1}$ ) in water/DMF (4:1, v/v) solution at three different pH values

lacks the amine receptor at the 4-amino moiety, did not show any changes in the emission properties as a function of pH except at very low pH where the 4-amino moiety was protonated. The fluorescent enhancement (FE) was less than two times (FE=1.29).

Compounds **5** and **10**, containing secondary amine receptor at their 4-amino moieties, showed considerably higher fluorescence sensitivity as a function of pH. As a typical example of the two dyes, in basic solution for compound **5** only a weak emission was observed between 450 and 650 nm with maximum at  $\lambda_F=546$  nm. However, upon acidification the emission was gradually increased with the decrease of the pH value as demonstrated in Fig. 5. After careful titration to pH ca. 2.0, the emission maximal had shifted to 533 nm, and the emission intensity had enhanced approximately five times (FE=4.72). The fluorescent enhancement of compound **10** was FE=3.91. These changes are of such magnitude that they can be considered as representing two different “states”, where the fluores-

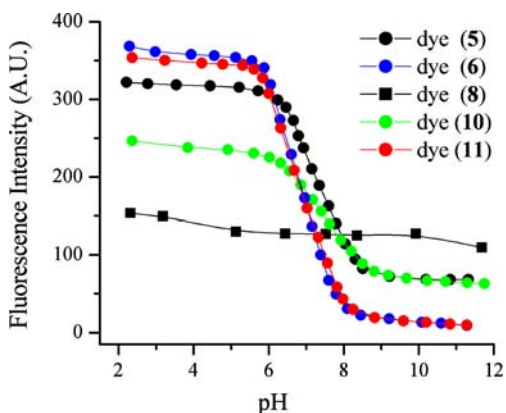


**Fig. 4** Effect of pH on the fluorescence intensity of compounds **5**, **6**, **8**, **10** and **11** in water/DMF (4:1, v/v)

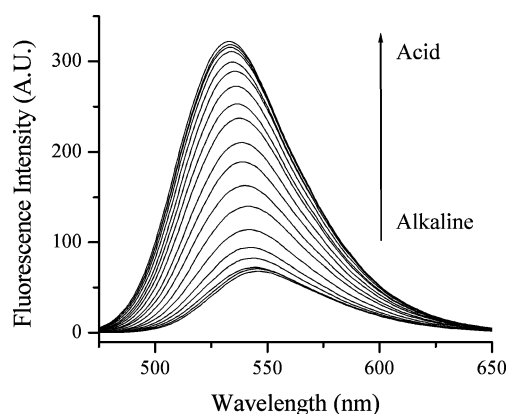


**Fig. 5** Changes in the fluorescence spectra of **5** as a function of pH in water/DMF (4:1, v/v). The pH range was from 11.32 to 2.21

cence emission is “switched off” in alkaline solution and “switched on” in acidic solution.

As can be seen (Schemes 1 and 2), compound **5** contains both “upper” and “lower” amine receptors, while compound **10** lacks “upper” amine receptor. Nevertheless, the fluorescent enhancement values of compounds **5** and **10** as a function of pH are rather closed. That is why the fluorescence enhancement of compounds **5** and **10** can be attributed to protonation of the “lower” amine receptor in acidic medium. In alkaline solution this amine is engaged in PET quenching of the 1,8-naphthalimide excited state, and upon its protonation the quenching process is substantially removed (Scheme 5).

Whereas compounds **5** and **10** showed considerable changes in their emission properties as a function of pH, the fluorescence enhancement of compounds **6** and **11** is remarkable (Fig. 4) under the same conditions. Figure 6 presents as an example fluorescence changes of dye **6** over a wider pH scale. As seen protonation of the alkylated amine donor (receptor) in compound **6** drastically alters the

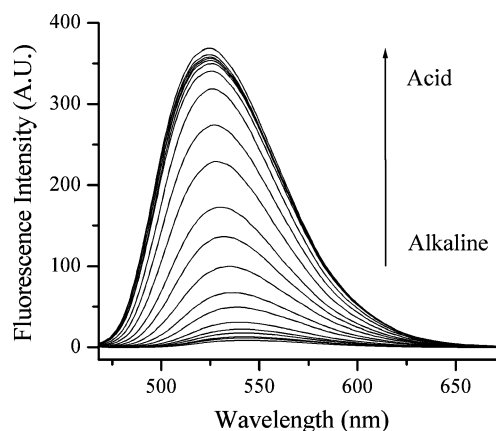


**Fig. 6** Changes in the fluorescence spectra of **6** as a function of pH in water/DMF (4:1, v/v). The pH range was from 11.28 to 2.29



electron-donating properties and consequently switching of the PET path from the alkylated amine donor to the 4-amino-1,8-naphthalimide moiety. The typical naphthalimide emission band of **6** in water/DMF (4:1, v/v) is blue-shifted upon-protonation and red-shifted upon deprotonation. Compared with the fluorescence in the basic medium, protonation of the alkylated amine of the novel dye **6** results in the fluorescence enhancement of the 4-amino-1,8-naphthalimide fluorophore by 41.89 times. Fluorescence enhancement of compound **11** was FE=36.33. The small difference in the FE values of compounds **6** and **11** shows that the protonation of the outer rim tertiary amine is responsible for the main part of the fluorescence enhancement.

In conclusion, novel 1,8-naphthalimides **5** and **6** are efficient “off-on” switchers for pH and the switching process was also found to be reversible. However the FE value of piperazine derivative **6** is fairly higher. Obviously, the oxidation potential of the secondary amine receptor (compounds **5** and **10**) increases quite less than that of the tertiary amine receptor (compounds **6** and **11**) after protonation of the amino moieties, and as such, thermodynamically disallows the electron transfer to a lower extent.

Taking the part of the graphs located between pH 5.5 and 9.0, the pH influence on the fluorescence intensity ( $I_F$ ) has been calculated by Eq. 5 [44]:

$$\log[(I_{F_{\max}} - I_F)/(I_F - I_{F_{\min}})] = \text{pH} - \text{p}K_a. \quad (5)$$

$\text{p}K_a$  values of 7.26–7.37 for dyes **5** and **10** and 6.92–6.96 for dyes **6** and **11** have been found. The results obtained are consistent with compounds of similar nature that were developed before [32, 41, 43]. These  $\text{p}K_a$  values also indicate that the novel sensors **5** and **6** would be well suited to monitor changes in the physiological pH range.

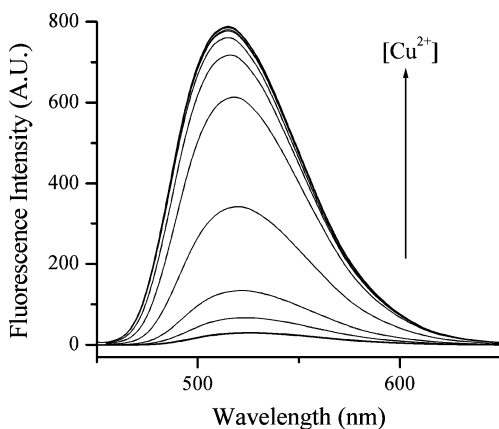


**Fig. 7** Fluorescence spectra of dye **6** ( $10^{-5}$  mol  $\text{l}^{-1}$ ) in DMF solution at various concentrations of  $\text{Cu}^{2+}$ . The concentrations of  $\text{Cu}^{2+}$  ions are in order of increasing intensity from 0 to  $3.33 \times 10^{-5}$  mol  $\text{l}^{-1}$  with step of  $3.33 \times 10^{-6}$  mol  $\text{l}^{-1}$

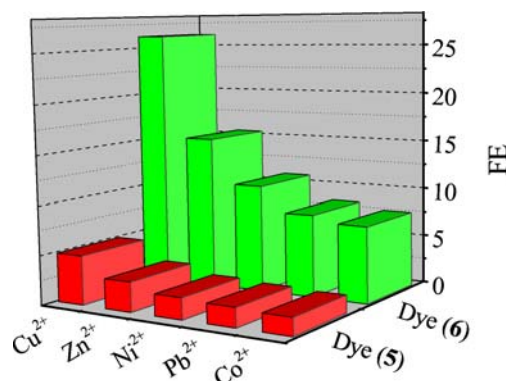


**Fig. 8** Fluorescence enhancement (FE) of 1,8-naphthalimides **5** and **6** ( $10^{-5}$  mol  $\text{l}^{-1}$ ) in the presence of different metal cations at concentration  $3.33 \times 10^{-5}$  mol  $\text{l}^{-1}$  in DMF solution

Influence of metal cations on the fluorescence intensity of the dyes

The signaling fluorescent properties of novel dyes **5** and **6** in the presence of transition metal ions have been investigated spectrophotometrically in DMF with regard to their potential application as PET sensors. DMF has been chosen in all measurements since it is able as a polar solvent to stabilize the dye charge separated state thus favoring the fluorescence switching by PET process. Also DMF guarantees a good solubility of the dye ligands, used metal salts and the respective complexes.

The fluorescence behaviour of the novel compounds (**5** and **6**) throughout the coordination process with different metal ions ( $\text{Cu}^{2+}$ ,  $\text{Pb}^{2+}$ ,  $\text{Zn}^{2+}$ ,  $\text{Ni}^{2+}$ ,  $\text{Co}^{2+}$ ) was, as expected, approximately the same as that in the presence of protons. It was found that the coordination of the dye receptor with the metal ion results in fluorescence enhancement, as it is demonstrated as an example in Fig. 7 for the piperazine substituted 1,8-naphthalimide **6** in the presence of  $\text{Cu}^{2+}$  ions.

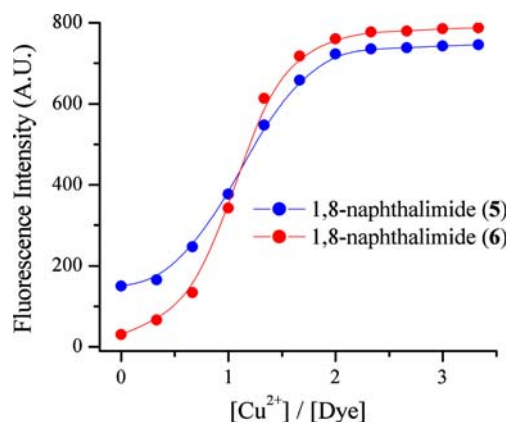
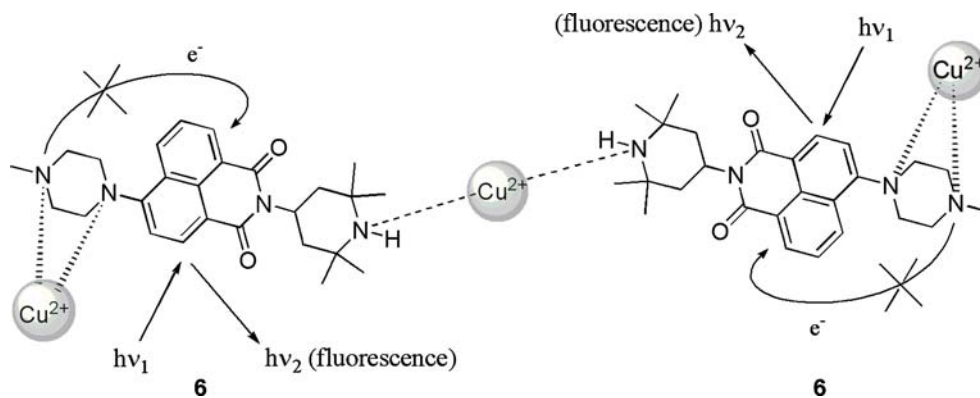


**Fig. 9** Changes in the fluorescence maxima of dyes **5** and **6** upon addition of  $\text{Cu}^{2+}$  ions

**Scheme 6** The observed hypsochromic shift of the dyes fluorescence maxima in the presence of metal ions indicating a bidentate chelation to both nitrogen atoms in the “lower” piperidine or piperazine moiety, as it is shown as an example for compound **6**



The sensor capacity of the fluorescent dyes **5** and **6** in respect to different metal ions and their concentration was evaluated on the basis of fluorescence enhancement values (Fig. 8). The  $FE=I/I_0$  was calculated using minimal ( $I_0$ ) and maximal ( $I$ ) fluorescence intensity recorded before and after addition of metal ions. The highest fluorescence enhancement of dyes **5** and **6** has been observed in the presence of  $\text{Cu}^{2+}$  ions ( $FE=4.98$  and  $26.22$ , respectively). As it is seen (Fig. 8), the  $FE$  values for compound **6** in the presence of all types of metal cations are about five times higher as compared to those of compound **5**, which could be related to the shorter hydrocarbon spacer and more pronounced increase in the oxidation potential of the tertiary amine receptor as already discussed in the “Influence of metal cations on the fluorescence intensity of the dyes” section (vide supra).

The increase in fluorescence intensity was occurred after addition of  $\text{Cu}^{2+}$  ions in the concentration range of  $3.33 \times 10^{-6}$  to  $3.33 \times 10^{-5} \text{ mol l}^{-1}$ . Noticeable fluorescence intensity enhancement was observed at  $\text{Cu}^{2+}$  concentration of  $6.67 \times 10^{-6} \text{ mol l}^{-1}$  which showed good sensitivity of the dyes (Fig. 9). Raising the cation concentration up to  $2.00 \times 10^{-5} \text{ mol l}^{-1}$  also induced an increase in the fluorescence. Further augmentation of the metal ions concentration up to  $3.33 \times 10^{-5} \text{ mol l}^{-1}$  had a small impact on the alteration of fluorescence intensity.

As discussed above, the fluorescence intensity increases due to the complexation between the piperidine (compound **5**) or piperazine (compound **6**) amine receptor and  $\text{Cu}^{2+}$  ions. However titration plots (Fig. 9) suppose a 3:2 metal/ligand complex formation. In consent to this assumption, a hypsochromic shift ( $\Delta\lambda_F=10\text{--}11 \text{ nm}$ ) of the dyes fluorescence maxima in the presence of metal ions has been observed, which indicates a bidentate chelation to both nitrogen atoms in the “lower” piperidine or piperazine moiety, as it is shown as an example for compound **6** in Scheme 6.

This type of chelation has two different effects: (1) the photoinduced electron transfer from the receptor amine to the fluorophore is disallowed causing a dye fluorescence

enhancement; (2) the electron donating ability of the aromatic (donor) amine at 1,8-naphthalimide C-4 position is reduced, and as such, the fluorescence maxima of the dyes shift to the shorter wavelength.

The results obtained reveal a good sensor activity of the novel yellow–green emitting fluorophores, especially possessing tertiary amine receptor fluorescent dye **6**, indicating their potential as highly efficient “off–on” switches for transition metals with pronounced selectivity towards  $\text{Cu}^{2+}$  ions.

#### Photostability of dyes

The fluorescent dyes’ photostability is a very important characteristic with regard to their practical usage. To study the influence of 2,2,6,6-tetramethylpiperidine fragment on the photostability of the target dyes **5** and **6**, DMF solutions of the dyes were subjected to irradiation in a SUNTEST equipment for 10 h. In order to receive a more complete comparative picture of this influence 1,8-naphthalimide **11**, not containing a hindered amine fragment, and 1,8-naphthalimides **8** and **10**, not containing “upper” or “lower”

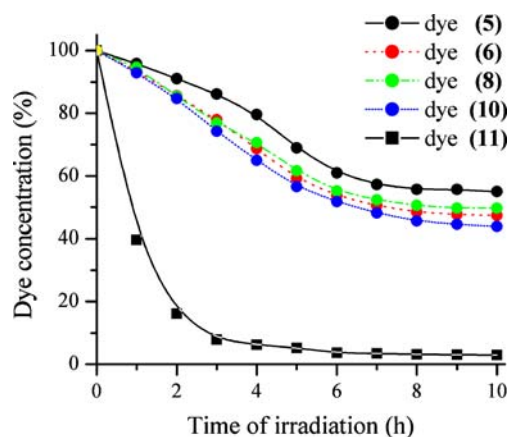


**Fig. 10** Photodegradation of 1,8-naphthalimides **5**, **6**, **8**, **10** and **11** in DMF solution

hindered amine moiety respectively (Scheme 2) were involved in the present study as reference compounds.

The kinetics of the dyes' photodegradation was monitored colorimetrically. As no changes were observed in the dyes absorption maxima ( $\lambda_A$ ) during the irradiation, the correlation between the dye concentration and the time of irradiation was monitored using the method of the standard calibration curve (Fig. 10).

As seen (Fig. 10), in DMF solution reference compounds **8** and **10**, containing "upper" or "lower" hindered amine fragment respectively, show high photostability. The outline of photodegradation curves of the two dyes is very close. Obviously the position effect of hindered amine moiety on the 1,8-naphthalimide photostability is negligible. In the case of dye **11**, not containing stabilizer unit in its molecule, the photodegradation was considerably faster if compared to those of dyes **8** and **10**. Within 2–3 h the dye **3** solution loses significant part of its absorption capacity as a result of photodegradation of the dye chromophoric system.

Photostability of the novel dye **6**, containing "upper" hindered amine fragment, is approximately the same as that of the reference analogue **8**, which is very well correlated with the structure propinquity of these compounds. Photostability of the novel dye **5**, containing both "upper" and "lower" hindered amine fragments, is slightly higher probably due to the participation of a second stabilizer moiety in the dye molecule.

The results obtained show that the novel compounds **5** and **6** are highly photostable dyes with high potential for use as effective fluorescence detectors of environmental pollution by metal ions and protons.

## Conclusions

In this paper we have given a comprehensive account of the design of two yellow–green emitting 4-amino-1,8-naphthalimide dyes, containing *N*-linked hindered amine moiety, as highly photostable PET fluorescence sensors for metal ions and protons. Their photophysical properties were studied in DMF and water/DMF (4:1, *v/v*) solution and discussed. Photooxidative stability of the new fluorophores was studied and compared to that of other similar fluorescent dyes, not containing hindered amine fragment in their molecules. It was shown that the presence of a hindered amine fragment in the dyes' molecules considerably improved their photostability. In the presence of metal ions ( $\text{Cu}^{2+}$ ,  $\text{Pb}^{2+}$ ,  $\text{Zn}^{2+}$ ,  $\text{Co}^{2+}$ ,  $\text{Ni}^{2+}$ ) and protons these molecules sustained appreciable changes in their fluorescence intensity. These changes can be attributed to coordination of their piperidine or piperazine amine receptor with the analyte, whereupon the receptor increases its oxidation potential, and as such, thermodynamically disallow the electron

transfer and the emission is "switched on". Compound **5**, containing secondary amine receptor, displayed a good sensor activity towards metal ions and protons. However the sensor activity of dye **6**, containing a tertiary amine receptor and a shorter hydrocarbon spacer, was substantially higher. The results obtained indicate the potential of the novel compounds as highly photostable and efficient "off–on" pH switchers and fluorescent detectors for metal ions with pronounced selectivity towards  $\text{Cu}^{2+}$  ions.

**Acknowledgements** This work was supported by the National Science Foundation of Bulgaria (project VU-X-201/06). Vladimir Bojinov and Nikolai Georgiev also acknowledge the Science Foundation at the University of Chemical Technology and Metallurgy (Sofia, Bulgaria).

## References

- Balzani V (2003) Photochemical molecular devices. *Photochem Photobiol Sci* 2:459–476 doi:10.1039/b300075n
- de Silva A, Fox D, Huxley A, Moody T (2000) Combining luminescence, coordination and electron transfer for signalling purposes. *Coord Chem Rev* 205:41–57 doi:10.1016/S0010-8545(00)00238-1
- Rurack K, Resch-Gender U (2002) Rigidization, preorientation and electronic decoupling—the magic triangle for the design of highly efficient fluorescent sensors and switches. *Chem Soc Rev* 31:116–127 doi:10.1039/b100604p
- Balzani V, Credi A, Raymo F, Stoddart J (2000) Artificial molecular machines. *Angew Chem Int Ed* 39:3348–3391 doi:10.1002/1521-3773(20001002)39:19<3348::AID-ANIE3348>3.0.CO;2-X
- Raymo F (2002) Digital processing and communication with molecular switches. *Adv Mater* 14:401–414 doi:10.1002/1521-4095(20020318)14:6<401::AID-ADMA401>3.0.CO;2-F
- He H, Mortellaro M, Leiner M, Young S, Fraatz R, Tusa J (2003) A fluorescent chemosensor for sodium based on photoinduced electron transfer. *Anal Chem* 75:549–555 doi:10.1021/ac0205107
- Gunnlaugsson T, Bichell B, Nolan C (2002) A novel fluorescent photoinduced electron transfer (PET) sensor for lithium. *Tetrahedron Lett* 43:4989–4992 doi:10.1016/S0040-4039(02)00895-X
- Bissell R, de Silva A, Gunaratne H, Lynch P, Maguire G, McCoy C et al (1992) Molecular fluorescent signalling with fluorophore–spacer–receptor systems: approaches to sensing and switching devices via supramolecular photophysics. *Chem Soc Rev* 21:187–196 doi:10.1039/cs9922100187
- de Silva A, Gunaratne H, Gunnlaugsson T, Huxley A, McCoy C, Rademacher J et al (1997) Signaling recognition events with fluorescent sensors and switches. *Chem Rev* 97:1515–1566 doi:10.1021/cr960386p
- Valeur B, Leray I (2000) Design principles of fluorescent molecular sensors for cation recognition. *Coord Chem Rev* 205:3–40 doi:10.1016/S0010-8545(00)00246-0
- de Silva A, Fox D, Huxley A, McClenaghan N, Roiron J (1999) Metal complexes as components of luminescent signalling systems. *Coord Chem Rev* 186:297–306 doi:10.1016/S0010-8545(98)00275-6
- de Silva A, McCaughan B, McKinney B, Querol M (2003) Newer optical based molecular devices from older coordination chemistry. *Dalton Transactions* 10:1902–1913 doi:10.1039/b212447p

13. Callan J, de Silva A, Magri D (2005) Luminescent sensors and switches in the early 21st century. *Tetrahedron* 61:8551–8588 doi:10.1016/j.tet.2005.05.043
14. Gan J, Chen K, Chang CP, Tian H (2003) Luminescent properties and photo-induced electron transfer of naphthalimides with piperazine substituent. *Dyes Pigm* 57:21–28 doi:10.1016/S0143-7208(02)00162-6
15. de Silva A, Goligher A, Gunaratne H, Rice T (2003) The pH-dependent fluorescence of pyridylmethyl-4-amino-1,8-naphthalimides. *Arkivoc* 7:229–243
16. Patrick L, Whiting A (2002) Synthesis of some polymerisable fluorescent dyes. *Dyes Pigm* 55:123–132 doi:10.1016/S0143-7208(02)00067-0
17. Bojinov V, Konstantinova T (2002) Synthesis of polymerizable 1,8-naphthalimide dyes containing hindered amine fragment. *Dyes Pigm* 54:239–245 doi:10.1016/S0143-7208(02)00047-5
18. Bojinov V, Grabchev I (2003) Synthesis of new polymerizable 1,8-naphthalimide dyes containing a 2-hydroxyphenylbenzotriazole fragment. *Dyes Pigm* 59:277–283 doi:10.1016/S0143-7208(03)00113-X
19. Bojinov V, Panova I (2007) Synthesis and absorption properties of new yellow-green emitting benzo[de]isoquinoline-1,3-diones containing hindered amine and 2-hydroxyphenylbenzotriazole fragments. *Dyes Pigm* 74:551–560 doi:10.1016/j.dyepig.2006.03.016
20. Hrdlovič P, Chmela Š, Danko M (1998) Spectral characteristics and photochemical stability of fluorescence probes based on 1,8-naphthaleneimide in solution and in polymer matrix. *J Photochem Photobiol A Chem* 112:197–203 doi:10.1016/S1010-6030(97)00277-3
21. Kollar J, Hrdlovič P, Chmela Š (2008) Synthesis and spectral characteristics of di-substituted 1,8-naphthalimides: bi-radical formation. *J Photochem Photobiol A Chem* 195:64–71 doi:10.1016/j.jphotochem.2007.09.008
22. Hrdlovič P, Chmela Š, Danko M, Sarakha M, Guyot G (2008) Spectral properties of probes containing benzothioxanthene chromophore linked with hindered amine in solution and in polymer matrices. *J Fluoresc* 18:393–402 doi:10.1007/s10895-007-0279-9
23. Martin E, Weigand R, Pardo A (1996) Solvent dependence of the inhibition of intramolecular charge-transfer in *N*-substituted 1,8-naphthalimide derivatives as dye lasers. *J Lumin* 68:157–164 doi:10.1016/0022-2313(96)00008-7
24. Gruzinskii V, Kukhto A, Shakkah G (1998) Spectra of lasing efficiency in lasers with solutions of complex organic compounds. *J Appl Spectrosc* 65:463–465 doi:10.1007/BF02675471
25. Tao ZF, Qian X (1999) Naphthalimide hydroperoxides as photonucleases: substituent effects and structural basis. *Dyes Pigm* 43:139–145 doi:10.1016/S0143-7208(99)00037-6
26. Stewart W (1981) Synthesis of 3,6-disulfonated 4-aminonaphthalimides. *J Am Chem Soc* 103:7615–7620 doi:10.1021/ja00415a033
27. Morgado J, Gruner J, Walcott SP, Yong TM, Cervini R, Moratti SC et al (1998) 4-AcNI—a new polymer for light-emitting diodes. *Synth Met* 95:113–117 doi:10.1016/S0379-6779(98)00042-3
28. Zhu W, Hu C, Chen K, Tian H (1998) Luminescent properties of copolymeric dyad compounds containing 1,8-naphthalimide and 1,3,4-oxadiazole. *Synth Met* 96:151–154 doi:10.1016/S0379-6779(98)00083-6
29. Tian H, Gan J, Chen K, He J, Song Q, Hou X (2002) Positive and negative fluorescent imaging induced by naphthalimide polymers. *J Mater Chem* 12:1262–1267 doi:10.1039/b200509c
30. Grabchev I, Qian X, Bojinov V, Xiao Y, Zhang W (2002) Synthesis and photophysical properties of 1,8-naphthalimide-labelled dendrimers as PET sensors of proton and transition metal ion. *Polymer (Guildf)* 43:5731–5736 doi:10.1016/S0032-3861(02)00417-2
31. Tian H, Xu T, Zhao Y, Chen K (1999) Two-path photo-induced electron transfer in naphthalimide-based model compound. *J Chem Soc Perkin Trans* 2:545–549 doi:10.1039/a808123i
32. Bojinov V, Konstantinova T (2007) Fluorescent 4-(2,2,6,6-tetramethylpiperidin-4-ylamino)-1,8-naphthalimide pH chemosensor based on photoinduced electron transfer. *Sens Actuators B Chem* 123:869–876 doi:10.1016/j.snb.2006.10.035
33. Poteau X, Brown A, Brown R, Holmes C, Matthew D (2000) Fluorescence switching in 4-amino-1,8-naphthalimides: “on–off–on” operation controlled by solvent and cations. *Dyes Pigm* 47:91–105 doi:10.1016/S0143-7208(00)00067-X
34. Jia L, Zhang Y, Guo X, Qian X (2004) A novel chromatism switcher with double receptors selectively for Ag<sup>+</sup> in neutral aqueous solution: 4,5-diaminoalkeneamino-*N*-alkyl-1,8-naphthalimides. *Tetrahedron Lett* 45:3969–3973 doi:10.1016/j.tetlet.2004.03.105
35. Zhu W, Hu M, Yao R, Tian H (2003) A novel family of twisted molecular luminescent materials containing carbazole unit for single-layer organic electroluminescent devices. *J Photochem Photobiol A Chem* 154:169–177 doi:10.1016/S1010-6030(02)00325-8
36. Facchetti H, Robin P, Le Barny P, Schott M, Bouche CM, Berdague P (1996) Side-chain electroluminescent polymers. *Synth Met* 81:191–195 doi:10.1016/S0379-6779(96)03767-8
37. Zhu W, Minami N, Kazaoui S, Kim Y (2003) Fluorescent chromophores functionalized single-wall carbon nanotubes with minimal alteration to their characteristic one-dimensional electronic states. *J Mater Chem* 13:2196–2201 doi:10.1039/b303885h
38. Grabchev I, Chovelon JM (2003) Synthesis and functional properties of green fluorescent poly(methylmethacrylate) for use in liquid crystal systems. *Polym Adv Technol* 14:601–608 doi:10.1002/pat.376
39. Grabchev I, Moneva I, Bojinov V, Guittonneau S (2000) Synthesis and properties of fluorescent 1,8-naphthalimide dyes for application in liquid crystal displays. *J Mater Chem* 10:1291–1296 doi:10.1039/a909153j
40. Cosnard F, Wintgens V (1998) A new fluoroionophore derived from 4-amino-*N*-methyl-1,8-naphthalimide. *Tetrahedron Lett* 39:2751–2754 doi:10.1016/S0040-4039(98)00302-5
41. Grabchev I, Sali S, Betcheva R, Gregoriou V (2007) New green fluorescent polymer sensors for metal cations and protons. *Eur Polym J* 43:4297–4305 doi:10.1016/j.eurpolymj.2007.07.036
42. Reynolds G, Drexhage K (1975) New coumarin dyes with rigidized structure for flashlamp-pumped dye lasers. *Opt Commun* 13:222–225 doi:10.1016/0030-4018(75)90085-1
43. de Silva A, Gunaratne H, McCoy C (1993) A molecular photoionic AND gate based on fluorescent signaling. *Nature* 364:42–44 doi:10.1038/364042a0
44. de Silva A, Gunaratne H, Habib-Jiwan JL, McCoy C, Rice T, Soumillion JP (1995) New fluorescent model compounds for the study of photoinduced electron transfer: the influence of molecular electric field in the excited state. *Angew Chem Int Ed Engl* 34:1728–1731 doi:10.1002/anie.199517281
45. Rurack K (2001) Flipping the light switch ‘ON’—the design of sensor molecules that show cation-induced fluorescence enhancement with heavy and transition metal ions. *Spectrochim Acta Part A Mol Biomol Spectrosc* 57:2161–2195
46. Gordon P, Gregory P (1987) *Organic chemistry in colour*. Springer, Berlin
47. Grabchev I, Bojinov V, Petkov H (2001) Synthesis and photophysical properties of polymerizable 1,8-naphthalimide dyes and their copolymers with styrene. *Dyes Pigm* 51:1–8 doi:10.1016/S0143-7208(01)00041-9

48. Yang S, Meng F, Tian H, Chen K (2002) Photostability of novel copolymers functionalized with laser dyes based on modified rhodamine 6G and 1,8-naphthalimide. *Eur Polym J* 38:911–919 doi:[10.1016/S0014-3057\(01\)00265-8](https://doi.org/10.1016/S0014-3057(01)00265-8)
49. Terenin A (1967) *Photonics of dyes and related organic compounds*. Science, Leningrad (in Russian)
50. Gunnlaugsson T, McCoy C, Morrow R, Phelan C, Stomeo F (2003) Towards the development of controllable and reversible ‘on–off’ luminescence switching in soft-matter; synthesis and spectroscopic investigation of 1,8-naphthalimide-based PET (photoinduced electron transfer) chemosensors for pH in water-permeable hydrogels. *Arkivoc* 7:216–228